

Thermoelectric Micro-Refrigerator Based on Bismuth/Antimony Telluride

LINH TUAN DANG,^{1,2} TUNG HUU DANG,^{1,2} THAO THI THU NGUYEN,¹
THUAT TRAN NGUYEN,² HUE MINH NGUYEN,³
TUYEN VIET NGUYEN,¹ and HUNG QUOC NGUYEN^{2,4}

1.—Faculty of Physics, VNU University of Science, 334 Nguyen Trai, Thanh Xuan District, Hanoi, Vietnam. 2.—Nano and Energy Center, VNU University of Science, 334 Nguyen Trai, Thanh Xuan District, Hanoi, Vietnam. 3.—Department of Physics, Le Quy Don Technical University, 236 Hoang Quoc Viet, Bac Tu Liem District, Hanoi, Vietnam. 4.—e-mail: hungngq@hus.edu.vn

Thermoelectric micro-coolers based on bismuth telluride (Bi_2Te_3) and antimony telluride (Sb_2Te_3) are important in many practical applications thanks to their compactness and fluid-free circulation. In this paper, we studied thermoelectric properties of bismuth/antimony telluride (Bi/SbTe) thin films prepared by the thermal co-evaporation method, which yielded among the best thermoelectric quality. Different co-evaporation conditions such as deposition flux ratio of materials and substrate temperature during deposition were investigated to optimize the thermoelectric figure of merit of these materials. Micron-size refrigerators were designed and fabricated using standard lithography and etching technique. A three-layer structure was introduced, including a *p*-type layer, an *n*-type layer and an aluminum layer. Next to the main cooler, a pair of smaller Bi/SbTe junctions was used as a thermocouple to directly measure electron temperature of the main device. Etching properties of the thermoelectric materials were investigated and optimized to support the fabrication process of the micro-refrigerator. We discuss our results and address possible applications.

Key words: Microfabrication, thermoelectric material, micro-device, thermoelectric micro-cooler

INTRODUCTION

Bismuth telluride (Bi_2Te_3) and antimony telluride (Sb_2Te_3) are two thermoelectric materials that attract great interest thanks to their high figures of merit (ZT),^{1,2} an essential property in refrigeration and power generation applications. Conventional macro-scale thermoelectric machines are commercially available and find their usages in many everyday applications. Nevertheless, a micro-thermal one is not yet available, despite tremendous attempts on fabricating a thermoelectric refrigerator.^{3–8}

The most important parameters of a thermoelectric material are the Seebeck coefficient (S), the

electrical conductivity (σ) and thermal conductivity (λ). They are related by a dimensionless figure of merit defined by Ref. 9:

$$ZT = \frac{\sigma S^2 T}{\lambda}. \quad (1)$$

The figure of merit can be improved by using alloy materials^{10,11} or engineering the nano- or micro-structure of the material (quantum wells, quantum wires, or half Heusler structures). In these low-dimensional systems, thin films are predicted to have lower thermal conductivity,^{12–15} and thus a micro-cooler should even outperform its bulk rival. The highest achieved ZT is 2.6, realized in a Bi_2Te_3 - Sb_2Te_3 superlattice.¹⁶

Another important parameter of the material is the power factor (PF), which determines the ability to transport heat (in a refrigerator) or generate energy (in a generator) of the material. It is given by Ref. 9:

$$PF = \sigma S^2. \quad (2)$$

Many thin film deposition techniques have been reported recently, leading to attempts to apply these techniques to the deposition of (Bi/Sb)Te thin film.^{17,18} The thermal co-evaporation method is one of the most attractive techniques, which not only requires simple equipment but also produces thin films with high figures of merit at a good deposition rate.¹⁹ Bi/Sb and Te are heated and vaporized in separated sources; their vapors mix at a fixed composition and condense into film on the substrate. Direct evaporation of bulk material (Bi_2Te_3 or Sb_2Te_3) is not recommended. These materials decompose, then Te and Bi/Sb evaporate at different rates, causing a gradient of composition, changing from Te-rich to Bi/Sb-rich vertically in the film.¹⁹

Focusing on the cooling ability of thermoelectric materials, we designed a micro-scale device that could test the actual cooling power of $\text{Bi}_2\text{Te}_3/\text{Sb}_2\text{Te}_3$ thin films deposited by the thermal co-evaporation method. Figure 1 shows the top view and planar view of the device. The working component is two $100 \times 100 \mu\text{m}^2$ thin films, with a p -type Sb_2Te_3 and an n -type Bi_2Te_3 film, providing the cooling power of the device. Two similar but smaller $10 \times 50 \mu\text{m}^2$ films of Sb_2Te_3 and Bi_2Te_3 form a thermocouple. They are about ten times smaller than the main junction so that the cooling power is miniscule. When the primary pair is biased with a current, the center region of the device is cooled, which is detectable using the secondary pair—the thermometer. Temperature difference between the cooled metal and its surroundings leads to a Seebeck voltage on the thermometer. In the side view, the device consists of three layers, deposited and fabricated separately and in sequence. The first layer is a p -type thin film, which is then patterned into a large primary junction and a small secondary junction. The second layer is n -type Bi_2Te_3 , fabricated similarly to the first layer that completes two thermocouples. The third layer is Al, which forms the electrical connects and contacts for the device.

EXPERIMENT

Thin Film Deposition

Bi_2Te_3 and Sb_2Te_3 thin films were deposited using a thermal co-evaporation method by using a 3-source evaporation system from Syskey Technology Co. Bi/Sb and Te were placed in two separated tungsten boats in two crucibles. A vacuum under 4×10^{-7} kPa was maintained during co-deposition

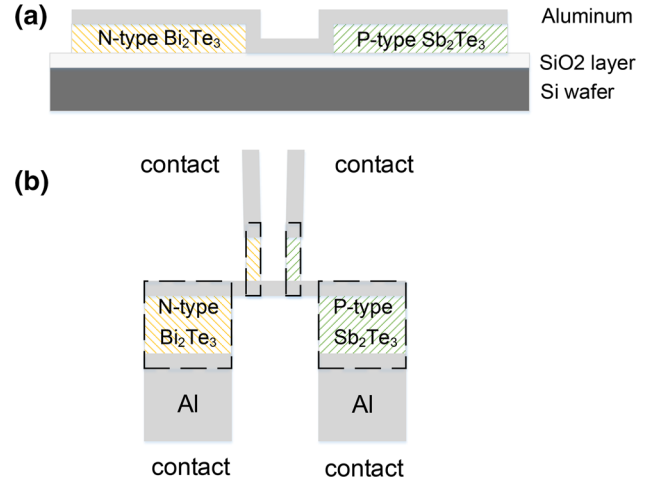


Fig. 1. (a) Side view of the micro-device: Bi_2Te_3 was first deposited and patterned using photolithography and chemical wet-etch. A second deposition and lithography created the Sb_2Te_3 layer. The final lithography step connected the p -type and n -type layer with 100 nm of Al. (b) Top view of the refrigerator: the two large junctions provided cooling power for the device. The two small junctions acted as an electronic thermometer.

process. All films were deposited on silicon chips of $1.5 \times 1.5 \text{ cm}^2$, which were cleaned with acetone—ethanol and piranha solution. Two quartz sensors were used to determine the deposition rate of each material separately. Both sensors were calibrated to measure the exact deposition rate at the substrate holder level. A metal (copper) shield was placed between the sources to prevent the mixing of the materials at the sensor level, so that each sensor would measure only the rate of one material.¹⁹ The ratio of Te deposition rate over Bi/Sb deposition rate (now referred to as FR) was recorded. The deposition rate of Bi/Sb was fixed at 1 Å/s when the deposition rate of Te was varied between 1.5 Å/s and 3 Å/s. The stability of deposition rates of the materials was significantly different. It was observed from the crystal sensors that when Bi and Te deposition rates fluctuated weakly (<0.05 Å/s for Bi, ~ 0.1 Å/s for Te), the deposition rate of Sb was much more unstable (~ 0.4 – 0.5 Å/s), mostly due to its sublimation property.²⁰ Rotation during deposition process helped improve the uniformity of the film, both thickness and composition distribution. An infrared heater system and a thermocouple were available to heat the substrate to the desired temperature. The thermal co-evaporation system is shown in Fig. 2.

Films quality was studied by first depositing material through a shadow mask, shown in Fig. 3, to create a structure that supports the Seebeck and Van der Pauw measurements. For the Van der Pauw measurement, the films were deposited in a common clover leaf shape.²¹ For the Seebeck measurement, the films consisted of six different $2 \times 2 \text{ mm}^2$ contacts. The two contacts at two ends of the figure were set at different temperatures

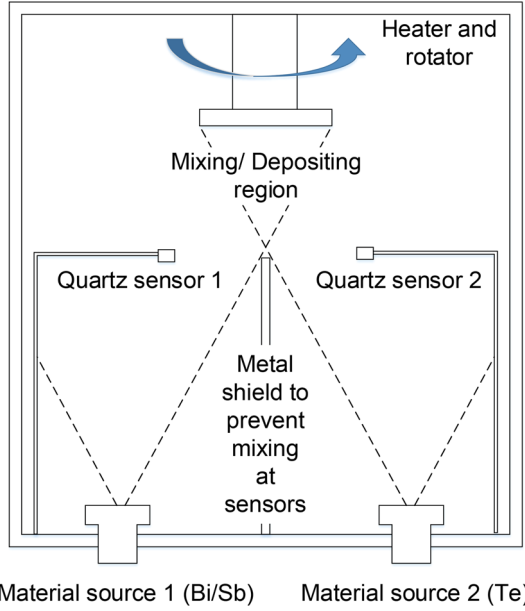


Fig. 2. Thermal co-evaporation chamber. Two separate sources of Bi(Sb) and Te were controlled by computer to achieve a precise ratio rate, which is measured by the two independent quartz crystals. The substrate rotated at 6 rounds per minute for better film uniformity.

during measurement (one hot end and one cold end), and the voltage was measured between them using two gold-coated contacts connected to Cu wires, where the other four contacts are for cross-checking. The Seebeck coefficient of the material was calculated by the formula:

$$S = -\frac{\Delta V}{\Delta T} + S_{Cu}, \quad (3)$$

where S is the Seebeck coefficient of the material, ΔV is the voltage between the hot side and cold side, ΔT is the temperature difference between two sides and $S_{Cu} = 1.83$ ($\mu\text{V}/\text{K}$) is the Seebeck coefficient of the Cu wire.²² Two ends of the sample were mounted on two bronze heat sinks using a thermal-conductive grease. The heat sinks were connected to two conventional thermoelectric coolers (TECs). The hot bronze block was connected to the hot side of a TEC, while the cold end was connected to the cold side of another TEC, and the TECs were mounted on an aluminum heat sink for better thermalization. When applied with a current, the two TECs would function as a heat pump, dissipating heat from the cold bronze block to the hot one and maintaining a temperature gradient between the two ends of the sample. Two Pt-100 temperature sensors attached to the bronze blocks measured the temperature difference. Figure 4 shows the top view and side view of our Seebeck measurement system.

Micro-device Fabrication

The structure presented above was fabricated with p -type Sb_2Te_3 film and n -type Bi_2Te_3 , both

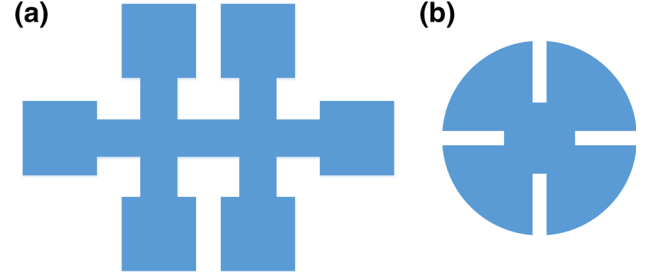


Fig. 3. Shadow masks were micro-machined from a piece of aluminum that allowed basic characterization of the thin film. Design for (a) Seebeck coefficient measurement and (b) Van der Pauw measurement.

with thickness of 200 nm, importing fabrication techniques from MEMS fabrication. Sb_2Te_3 films were deposited with $FR = 2.5$ (Te:Sb) and a substrate temperature of 250°C during deposition. The respective parameters for Bi_2Te_3 are 3 (Te:Bi) and 300°C . Thermoelectric thin films were first deposited on a silicon substrate with a thin layer of SiO_2 followed by a $1.4 \mu\text{m}$ -layer of AZ-5214E photoresist by spin-coating. The film was then exposed to UV radiation of dose $150 \text{ mJ}/\text{cm}^2$ using a standard UV photolithography system. A developing process in tetramethylammonium hydroxide (TMAH) would then pattern the photoresist layer, followed by a wet-etching process to pattern the thermoelectric film. The etchants were diluted in aqua regia solution (3:1 HNO_3 :HCl in volume) for Sb_2Te_3 film and diluted nitric acid for Bi_2Te_3 , thanks to the reported selective etching property of HNO_3 .^{19,23} The aluminum (Al) connecting wires in the device were fabricated by evaporation, photolithography and then wet-etching.²⁴

RESULTS AND DISCUSSION

Thermoelectric Thin Films

We first studied the dependence of thermoelectric properties of Sb_2Te_3 and Bi_2Te_3 as a function of FR. Figure 5 demonstrates the measured Seebeck voltage versus temperature differences. The temperature difference was calculated from the resistance difference of two calibrated Pt-100 thermistors:

$$\Delta T = \frac{R_1 - R(0)_1}{\alpha_1} - \frac{R_2 - R(0)_2}{\alpha_2}, \quad (4)$$

where R_1 and R_2 were the measured resistances, $R(0)_1$ and $R(0)_2$ was the resistance at 0°C , α_1 and α_2 were the temperature coefficient of resistance of the hot and cold thermistor, respectively.

The PF s of the samples were calculated from the Seebeck coefficient and resistivity as in formula (2). The highest PF obtained for Sb_2Te_3 thin film was $1.15 \times 10^{-3} \text{ W}/\text{mK}^{-2}$ at $FR = 1.5$. The PF was also high at $FR = 2.5$ ($0.94 \times 10^{-3} \text{ W}/\text{mK}^{-2}$), but relatively low for $FR = 2$ and 3 (0.0054×10^{-3} and 0.00016×10^{-3} respectively). For the Bi_2Te_3 film,

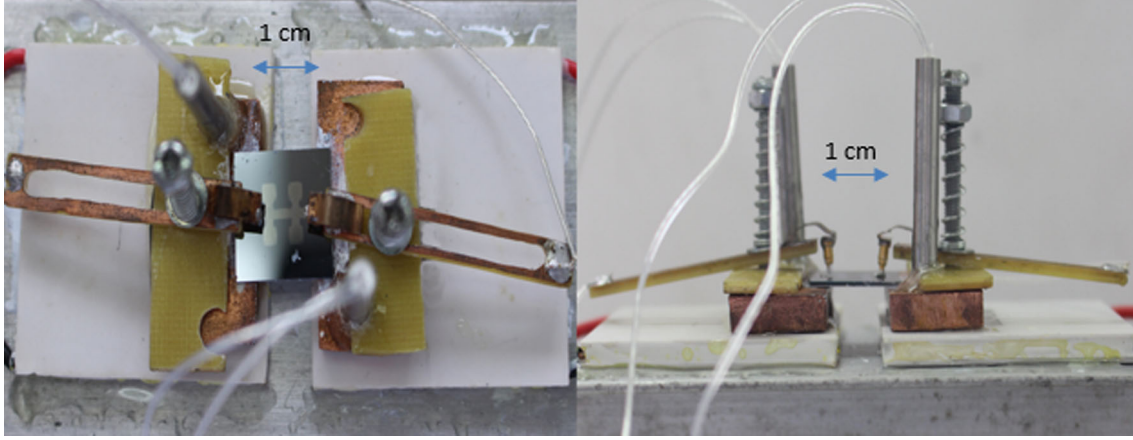


Fig. 4. Homemade Seebeck coefficient measurement setup: The silicon chip was held by two Cu clamps for good thermal conductance. These clamps sat on two Cu blocks, with temperature measured by a standard Pt100 thermocouple. The Cu blocks allowed a uniform thermal distribution on the Si chip. Heating and cooling of these bulky blocks were driven by two commercial thermal electric coolers, which resided on blocks of aluminum for better thermalisation.

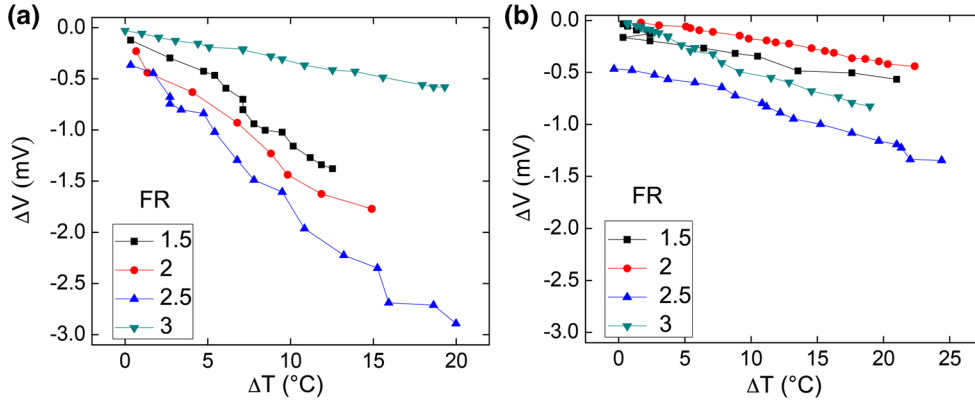


Fig. 5. Voltage difference versus temperature difference of (a) Sb_2Te_3 and (b) Bi_2Te_3 samples measured from the Seebeck coefficient measurement system.

the best PF was obtained with $FR = 2.5$ ($0.042 \times 10^{-3} \text{ W/mK}^{-2}$). The PF of Bi_2Te_3 increased as the composition was richer in Te, and reached maximum at $FR = 2.5$. The result is shown in Fig. 6.

Figure 7 shows the carrier concentration and mobility of Sb_2Te_3 and Bi_2Te_3 thin films prepared with different values of FR . The carrier concentration exhibited a similar trend as the power factor for Sb_2Te_3 films, which was high for $FR = 1.5$ and 2.5 (1.03×10^{21} and 1.6×10^{21} , respectively), and low for 2 and 3 (2.95×10^{16} and 7×10^{18}). For Bi_2Te_3 films, the highest concentration was achieved at $FR = 2$ (4.83×10^{21}), and Bi_2Te_3 film was a n -type for $FR = 1.5$, and a p -type for higher Te composition. The mobility of both materials varied very slightly around the value 2, except for $FR = 3$ with Sb_2Te_3 (very high value: 56.31) and $FR = 2$ with Bi_2Te_3 (low value: 0.35).

To study the effect of substrate temperature on the crystallization of thermoelectric thin films, we deposited Sb_2Te_3 and Bi_2Te_3 thin films at different substrate temperatures. The substrate was first

heated to the desired temperature, followed by film deposition. Sb_2Te_3 films with $FR = 2.5$ and Bi_2Te_3 with $FR = 3$ were deposited at room temperature, 250°C and 300°C . Figure 8 illustrates the diffractogram of Sb_2Te_3 and Bi_2Te_3 obtained by x-ray diffraction (XRD). Bi_2Te_3 films deposited at 300°C had the sharpest and highest peaks, while films deposited at 250°C showed a better crystallization than at room temperature. For Sb_2Te_3 films, the best crystallization was obtained at 250°C , while films deposited at 300°C and room temperature, showed a similar XRD diffractogram.

Micro-device Patterning

The etch rate of Bi_2Te_3 and Sb_2Te_3 in diluted aqua regia solution (3:1 HNO_3 : HCl in volume) was studied. Pure acids were used in the solution (68% HNO_3 and 37% HCl). P -type Sb_2Te_3 thin films were deposited at $FR = 2.5$ and substrate temperature 250°C , when n -type Bi_2Te_3 films were deposited at $FR = 3$ and substrate temperature 300°C . Etch

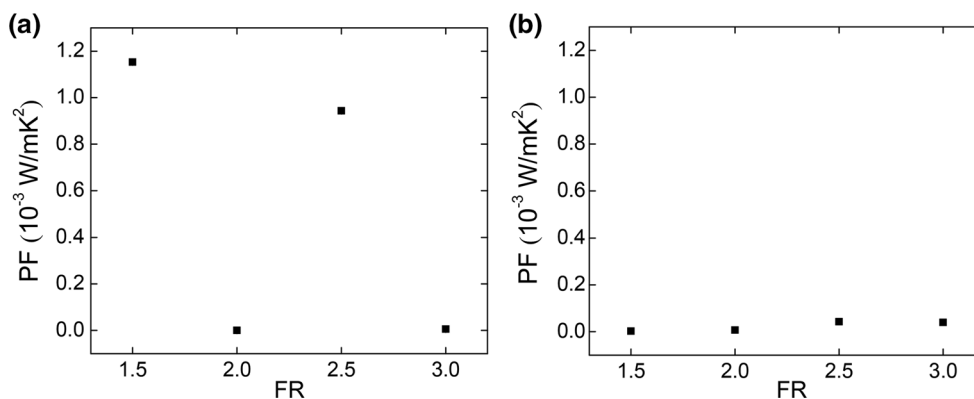


Fig. 6. Power factor of thermoelectric thin film calculated from Eq. 2 for various deposition ratios. All films are deposited at room temperature. (a) Sb_2Te_3 and (b) Bi_2Te_3 .

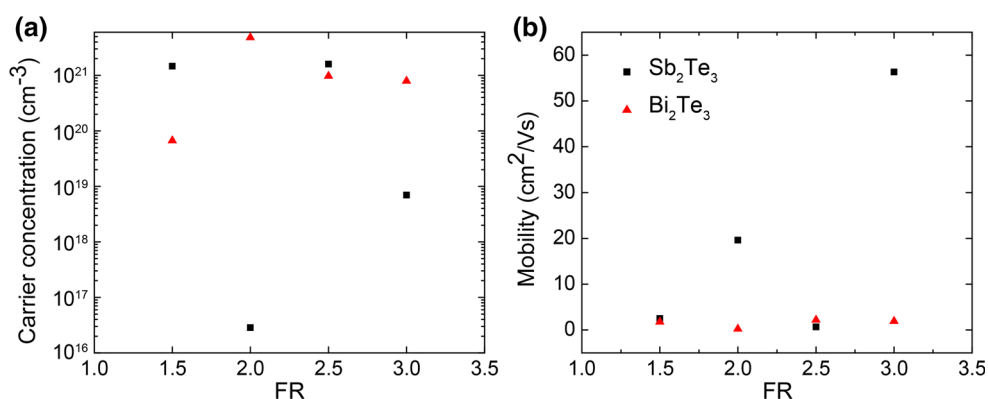


Fig. 7. (a) Carrier concentration and (b) mobility of Sb_2Te_3 and Bi_2Te_3 thin films.

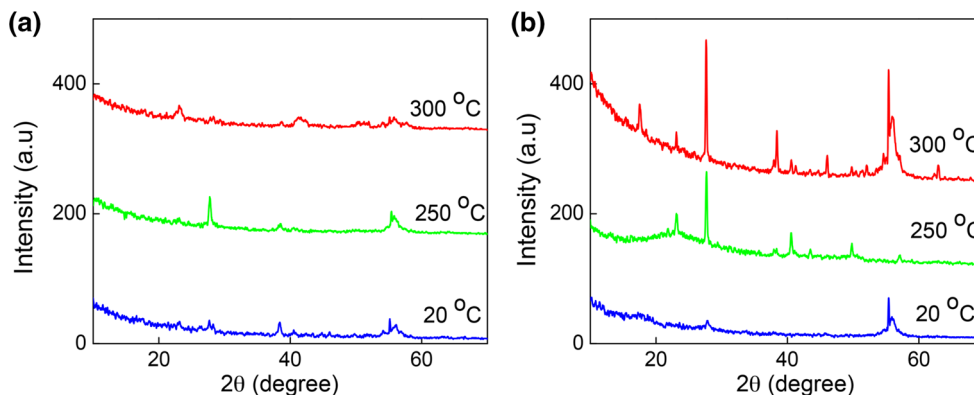


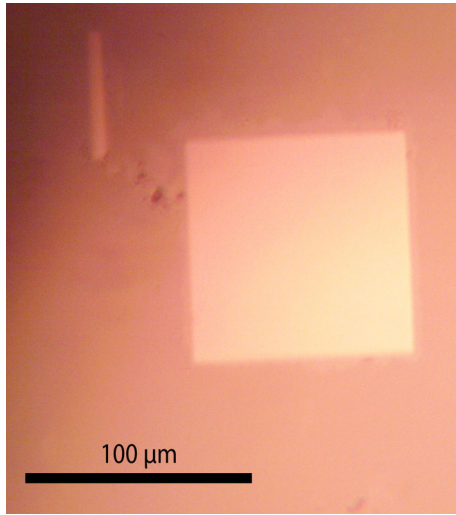
Fig. 8. X-ray diffraction data for (a) Sb_2Te_3 and (b) Bi_2Te_3 thin film at different substrate temperatures. The higher the temperature, the better visibility of the peak, which indicated crystalline thin films.

times of 200 nm thermoelectric films are shown in Table I. For concentration of acid greater than 50%, all films were quickly stripped off from the substrate and left no pattern on the substrate. Controllable etching was achieved with the concentration of acid less than 50%. For concentration less than 10%, the etch rate was slow, which led to peeling of the films. Good etch rates were achieved if acid concentration

was between 20% and 30%. However, etch time should be carefully controlled, otherwise small patterns such as the secondary thermocouple patterns and the alignment marks would be over-etched and left only the $100 \times 100 \mu m^2$ pattern on the substrate. This was partially due to the anisotropy properties of Sb_2Te_3 and Bi_2Te_3 thin films, which led to not only vertical but also

Table I. Etch rate of Bi/SbTe thin film in diluted aqua regia solution of different concentrations

Aqua regia concentration in water (%)	Etch time of 200 nm Sb ₂ Te ₃ (s)	Etch time of 200 nm Bi ₂ Te ₃ (s)	Note
100 (pure)	<1	<1	Fast, no pattern
50	12	10	Fast, no pattern
40	75	100	Normal, pattern observed
30	250	276	Normal, good pattern (Sb ₂ Te ₃)
20	375	350	Normal, good pattern (Sb ₂ Te ₃)
10	600	710	Slow, peeling

Fig. 9. Pattern of the first lithography step: Sb₂Te₃ thin film after 5 min wet-etching in HNO₃:HCl.

horizontal etching process, reducing the adhesion of the films on the substrate.

The first layer of *p*-type Sb₂Te₃ thin film was successfully fabricated using the prescribed recipe. After deposition and the patterning of the photoresist, the film was etched in 20% aqua regia solution in approximately 350 s (varying lightly among different samples). The photoresist was then removed by acetone, leaving the desired structure. Patterning of the second layer posed more difficulties, mostly due to the etchant attacking the patterned first layer and destroying the structure, even with the selective etching using HNO₃ for Bi₂Te₃ thin film. Figure 9 is an image of the *p*-type Sb₂Te₃ layer taken with an optical microscope. The primary thermocouple element (100 μm), the secondary thermocouple element and the alignment mark at the top left corner remain in good shape and size after etching and removing of photoresist.

CONCLUSIONS

In short, we have investigated the thermoelectric properties of thermoelectric thin films deposited by a thermal co-evaporation method and studied the

fabrication process of a thermoelectric micro-refrigerator. Deposition flux ratio of the materials affects greatly the electrical and thermoelectric properties of the materials. Best power factors are: $1.15 \times 10^{-3} \text{ W/mK}^{-2}$ obtained at $FR = 1.5$ for Sb₂Te₃ and $0.042 \times 10^{-3} \text{ W/mK}^{-2}$ at $FR = 2.5$ for Bi₂Te₃. Substrate heating during deposition is critical for the crystal structure of the film. The best crystallization is achieved at a substrate temperature of 250°C for Sb₂Te₃ and 300°C for Bi₂Te₃ films. Aqua regia solution is a good etchant for Bi₂Te₃ and Sb₂Te₃ thin film in the fabrication process of a micro-refrigerator. A concentration of 20–30% in water yields good results in etching the *p*-type Sb₂Te₃ layer, and a good pattern of this layer is successfully fabricated.

ACKNOWLEDGEMENTS

We acknowledge the support from the National Foundation for Science and Technology Development through Grant Number 103.02-2015.79. Samples were fabricated and measured at the Nano and Energy Center and Faculty of Physics, VNU University of Science. We would like to thank Mr. Nguyen Minh Hieu, Nano and Energy Center and Dr. Pham Van Thanh, Faculty of Physics for their support in the project.

REFERENCES

1. C.B. Satterthwaite and R.W. Ure Jr., *Phys. Rev.* 108, 1164 (1957).
2. X. Yan, B. Poudel, Y. Ma, W.S. Liu, G. Joshi, H. Wang, Y. Lan, D. Wang, G. Chen, and Z.F. Ren, *Nano Lett.* 10, 3373 (2010).
3. G.J. Snyder, J.R. Lim, C.K. Huang, and J.P. Fleurial, *Nat. Mater.* 2, 528 (2003).
4. J.R. Lim, G.J. Snyder, C. K. Huang, J.A. Herman, M.A. Ryan, and J.P. Fleurial, in *Proceedings of the 21st International Conference on Thermoelectrics*, IEEE, Long Beach, CA (2002).
5. W. Wang, F.J. Wei, F.Q. Huang, and J. Zhang, *Microelectron. Eng.* 77, 223 (2005).
6. L.M. Gonçalves, J.G. Rocha, C. Couto, P. Alpuim, G. Min, D.M. Rowe, and J.H. Correia, *J. Micromech. Microeng.* 17, S168 (2007).
7. J.P. Carmo, L.M. Gonçalves, J.H. Correia, and I.E.E.E.T. Ind, *Electron.* 57, 861 (2010).
8. H. Bottner, in *Proceedings of the Twenty-First International Conference on Thermoelectrics, ICT'02* (IEEE, 2002), p. 511.

Thermoelectric Micro-Refrigerator Based on Bismuth/Antimony Telluride

9. D.M. Rowe, ed., *CRC Handbook of Thermoelectrics*, (Boca Raton: CRC Press, 1995).
10. B. Poudel, Q. Hao, Y. Ma, Y. Lan, A. Minnich, B. Yu, and X. Yan, *Science* 320, 634 (2008).
11. S.R. Brown, S.M. Kauzlarich, F. Gascoin, and G.J. Snyder, *Chem. Mater.* 18, 1873 (2006).
12. L.D. Hicks and M.S. Dresselhaus, *Phys. Rev. B* 47, 12727 (1993).
13. L.D. Hicks, T.C. Harman, X. Sun, and M.S. Dresselhaus, *Phys. Rev. B* 53, R10493 (1996).
14. L.D. Hicks, T.C. Harman, and M.S. Dresselhaus, *Appl. Phys. Lett.* 63, 3230 (1993).
15. L.D. Hicks and M.S. Dresselhaus, *Phys. Rev. B* 47, 16631 (1993).
16. R. Venkatasubramanian, E. Siivola, T. Colpitts, and B. O'Quinn, *Nature* 413, 597 (2001).
17. H. Zou, D.M. Rowe, and S.G.K. Williams, *Thin Solid Films* 408, 270 (2002).
18. A. Giani, A. Boulouze, F. Pascal-Delannoy, A. Foucaran, E. Charles, and A. Boyer, *Mater. Sci. Eng. B* 64, 19 (1999).
19. L.M. Gonçalves, *The Deposition of Bi₂Te₃ and Sb₂Te₃ Thermoelectric Thin-Films by Thermal Co-evaporation and Applications in Energy Harvesting*, (Boca Raton: CRC Press, 2012).
20. H. Levinstein, *J. Appl. Phys.* 20, 306 (1949).
21. L.J. van der Pauw, *Philips Res. Rep.* 13, 1 (1958).
22. J. Blatt, *Thermoelectric Power of Metals*, (Berlin: Springer Science & Business Media, 2012).
23. C. Shafai and M.J. Brett, *Can. J. Phys.* 74, 139 (1996).
24. K.R. Kirt, K. Gupta, and M. Wasilik, *J. Microelectromech. S.* 12, 761 (2003).